

INELASTIC X-RAY SCATTERING IN CONDENSED MATTER SYSTEMS

Scattering experiments have given us much of what we know about the microscopic behavior of an enormous variety of condensed matter systems. Simple but fascinating materials such as solid and liquid helium, transition metals such as iron and nickel, semiconductors such as silicon and gallium arsenide, complex oxides such as V_2O_5 and high-temperature superconductors, and even more complex solids such as protein crystals have all been investigated by a variety of scattering probes.

The excitation energies of interest in condensed matter systems range from tens of electron volts down to tenths of millivolts, zero-energy transfer being a special case. The angular dependence of the scattering cross section in this zero-energy limit gives us the Fourier transform of the static spatial arrangement of the atoms making up the condensed matter system. In a perfect crystal, this scattering is called Bragg scattering.

Ultimately it is the excitations that tell us everything we want to know about the behavior of a system—its color, thermal properties, magnetic properties, electrical properties, phase characteristics and so on. Because of the enormous variety of excitations, ranging from phonons to plasmons to magnons, and because of the incredible range of momentum and energy scales of interest, different probes must be used. However, it is safe to say that neutrons and x rays have been the weak-scattering probes of choice for the study of condensed matter systems at atomic distance scales.

With very few exceptions, all x-ray scattering experiments in the last hundred years have been elastic scattering experiments. The elastic scattering of x rays is a coherent process, which means it is very intense and confined to certain angles. It is simple to observe with almost any source. Inelastic scattering, on the other hand, is weak, diffuse in angle and difficult to resolve, and only a very few research groups using available rotating anode sources are doing useful experiments. It has been clear for at least 20 years that new types of extremely bright, well-collimated tunable sources are necessary to perform such experiments.

When very-high-energy electrons are confined in an accelerator storage ring, they radiate enormous amounts of energy in a narrow, very-well-collimated beam. This synchrotron radiation has a broad energy spectrum extending into the hard x-ray region, is easily tunable and

Advances in synchrotron sources of hard x rays promise to open a new frontier in the use of inelastic scattering to probe eV and sub-eV electronic excitations in simple and complex solids and liquids.

Eric D. Isaacs and Phil Platzman

is polarized. In the last few years, synchrotron sources have created a revolution within the x-ray scattering community that is very much analogous to the revolution created by laser sources in the Raman scattering community. The original Raman experiments were done with mercury lamps and sunlight. The laser was much brighter and enabled one to perform new experiments in light scattering. Synchrotron sources are much brighter than conventional rotating anode sources and will also make possible new experiments with better resolution.

Kinematics

Scattering experiments use a beam of visible light, x rays, neutrons, electrons or other particles that have been monochromatized to a definite wavevector \mathbf{k}_1 , frequency ω_1 , polarization vector, spin and so on. The beam scatters into some final state specified, far from the sample, by \mathbf{k}_2 , ω_2 and so on. The momentum and energy transferred to the condensed matter system—that is, to the excitations—are $\hbar\mathbf{k} = \hbar(\mathbf{k}_2 - \mathbf{k}_1)$ and $\hbar\omega = \hbar(\omega_2 - \omega_1)$, respectively.

The range of momentum and energy transfer that can be probed in a given experiment is completely determined by kinematics—that is, by the energy and momenta of the initial and final beams. The maximum momentum transfer is always less than twice the momentum of the incident beam, whereas the minimum momentum transfer can be very small. The quantity k_{\min} is set by the smallest scattering angle θ that can be observed, because $k = 2k_1 \sin \theta/2$ and $k_1 = 2\pi/\lambda_1$. Here, $k = |\mathbf{k}|$.

The maximum energy transfer is clearly the incident energy, and the minimum is set by the energy resolution of the spectrometer and the brightness of the source. For elastic scattering, $\hbar\omega = 0$.

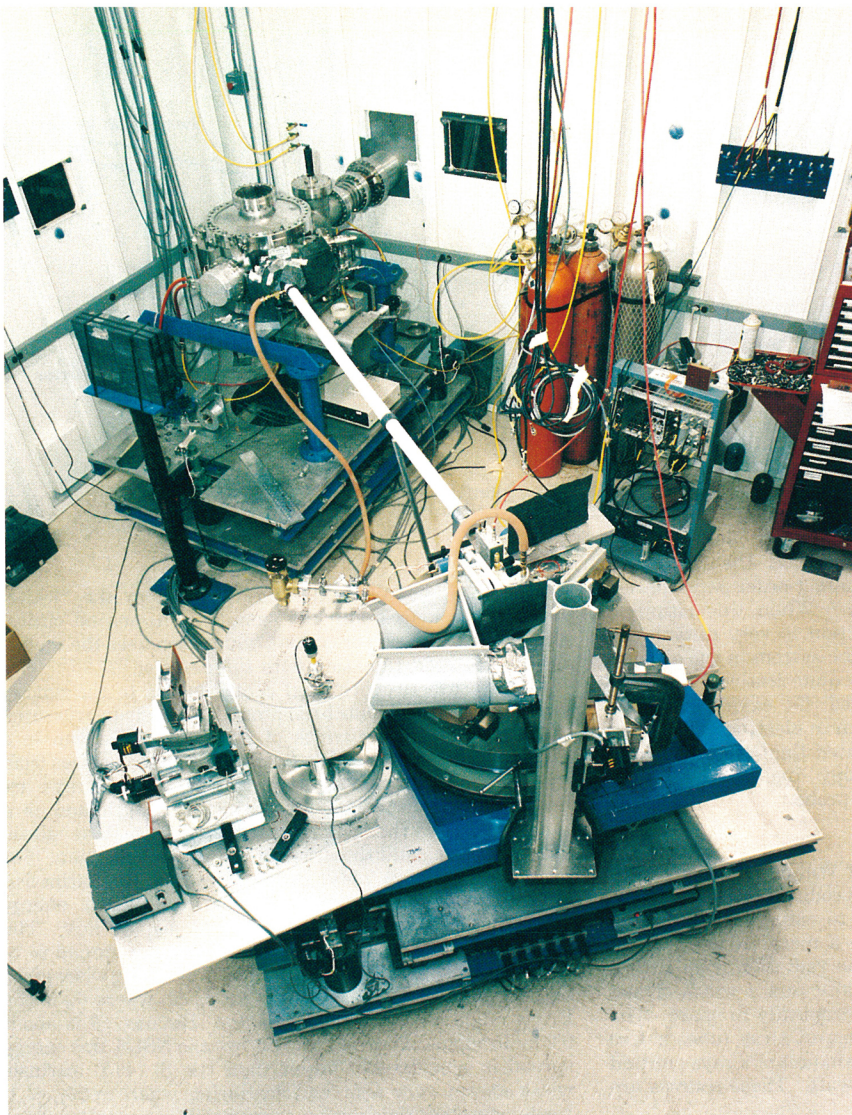
Elastic scattering is coherent, and therefore many amplitudes can add in phase if the momentum transfer is at some specific value $\hbar\mathbf{k} = \hbar\mathbf{k}_N$. Here, \mathbf{k}_N is a reciprocal lattice vector for a sample that is a perfect periodic crystal. Therefore, for a fixed energy and direction of the input beam, the cross section is very large. The output beam has the same energy as the input, and it exits at a fixed angle, called the Bragg angle θ_B , where

$$k_N = 2k_1 \sin \theta_B/2 \quad (1)$$

The size of the cross section and the spread in angle of the output beam depend on the number of atoms participating in the scattering, which is determined by the perfection of the crystal, by the extinction length of the x ray near the Bragg scattering energy and by the absorption of the x ray by the electrons of the solid.

In a typical solid there are, to a good approximation,

ERIC ISAACS and PHIL PLATZMAN are members of the technical staff at AT&T Bell Laboratories in Murray Hill, New Jersey.



BEAM LINE for inelastic x-ray scattering at the National Synchrotron Light Source, Brookhaven National Laboratory. FIGURE 1

two types of electrons: the outer, or valence, electrons whose low-lying excitations are of primary interest, and the core electrons, which are bound by energies of at least 100 eV. These core electrons dominate the elastic scattering and the absorption of the hard x rays. The fine structure on their high-energy excitation spectra (involving excitation of a core electron as well as some number of valence electrons) can be interesting, but is not central to the properties of the material.

For almost all solids, the density n of valence electrons is on the order of $10^{23}/\text{cm}^3$ and the mean free path $1/n\sigma_T$ for a nonresonant inelastic event is roughly 100 cm. (Here σ_T is the Thomson cross section per electron.) Because the absorption length for a 10-keV x ray in a typical transition metal such as nickel is 1 micron, the fraction of x rays scattered inelastically into 4π steradians is very small—approximately 10^{-6} . The small size of the inelastic cross section, its diffuse character in angle and energy, and the requirement of very high relative energy resolution make inelastic x-ray scattering measurements difficult. That is why so few experiments have been done and why we need new types of x-ray sources.

Neutrons have a very convenient kinematic match to the lengths and frequencies of interest in condensed matter. A neutron from a reactor has a typical energy of

10 meV and wavevector of $2 \times 10^8/\text{cm}$. Thus, it is relatively easy with modest energy and momentum resolution to probe a very relevant range of energy (0.1–10 meV) and wavevector transfer (2×10^6 – $10^9/\text{cm}$). If we compare this with light scattering, we immediately see the difference. For light scattering, $\hbar\omega_1 \approx 1$ eV and $k_1 \approx 10^5/\text{cm}$. Because of the extreme brightness (10^{18} photons/s) and coherence of laser sources, all relevant energies (10^{-15} eV $< \hbar\omega < 1$ eV) are accessible. Of course, the momentum transfer is limited to $k < 2 \times 10^5/\text{cm}$, which is quite small for most solids.

X rays typically have energies of 10 keV and momenta of $10^9/\text{cm}$. Thus, it is very easy to access any relevant wavevector transfers ($10^6 < k < 10^9/\text{cm}$) but difficult to access small energy transfers because the initial energy is so large. For example, an energy resolution of 0.01 percent gets us down to an energy transfer of about 1 eV, which is just barely relevant to the kind of energies we would like to access in condensed matter systems.

Inelastic x-ray scattering is arguably the only suitable probe of the electronic excitation spectrum at finite $\hbar\mathbf{k}$. Nevertheless, even though the discovery of x rays is now a century old, very few interesting inelastic x-ray scattering measurements have been performed. It is, in fact, quite easy to understand the reasons for this apparent

AN INELASTIC SCATTERING SPECTROMETER typically has three axes, defined by the two optical elements and the sample.

FIGURE 2

contradiction and to realize why we are now at the beginning of a new era. (See PHYSICS TODAY, November, 1995, pages 34 and 42 for other articles on x rays and condensed matter.)

In a so-called weak-scattering experiment, the coupling between the probe particles and the condensed matter system may be treated in lowest-order perturbation theory—the Born approximation. When this situation prevails, the scattering cross section is very directly related to a correlation function of the system in the absence of the probe. Accordingly, we may quantitatively interpret the data and avoid being plagued, for example, by the multiple scattering effects common in electron energy loss experiments or the strong unwanted final-state effects in photoemission and core spectroscopy. Inelastic x-ray scattering is such a weak-scattering probe.

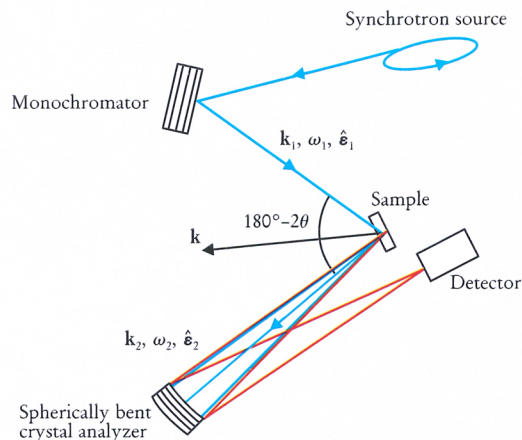
New x-ray sources

From the earliest experiments of Wilhelm Röntgen until very recently, x rays have been produced most easily by accelerating a beam of electrons to energies in excess of 20 keV and slamming them into a metal target such as copper.¹ The characteristic photon radiation from such a target has an energy of about 8 keV and a width of just 2.5 eV and is emitted roughly isotropically in space. The total power consumption of the biggest x-ray tubes is less than 100 kilowatts, and the total amount of x rays emitted into 4π steradians is less than 1 watt. These sources are not very bright.

Recently, electron storage rings have given us access to new, much brighter sources of x rays. (See PHYSICS TODAY, January 1994, page 18 and May 1995, page 59.) The relatively high brightness (photons/steradian/energy bandwidth) of these synchrotron sources² will make possible very good relative energy resolution— $\delta(\hbar\omega) \leq 0.1$ eV—over a broad range of absolute energy loss— $\hbar\omega < 10^3$ eV. At the same time, the high brightness will supply scientists with orders of magnitude more flux at the sample than is currently available from more conventional sources. The National Synchrotron Light Source at Brookhaven National Laboratory (figure 1) and the Advanced Light Source at Lawrence Berkeley National Laboratory (with softer x rays) are two of the major facilities. The next-generation facilities—namely, the European Synchrotron Radiation Facility in Grenoble, France; the Advanced Photon Source at Argonne National Laboratory; and SPring-8 near Himeji, Japan—are just coming on line. They will be even brighter sources of hard x rays.

Instrumentation

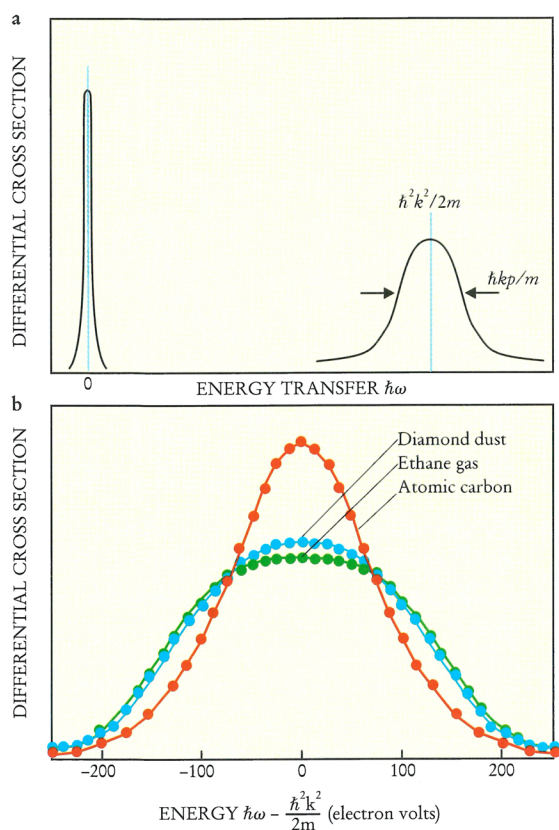
The inelastic scattering spectrometer (figure 2) is typically a three-axis instrument that contains two optical elements and a detector. The first element is the monochromator crystal, which passes a narrow, tunable energy band of



width $\delta(\hbar\omega_1)$ centered at energy $\hbar\omega_1$ from the “white” synchrotron source onto the sample. The second optical element is the analyzer crystal, which disperses the inelastically scattered radiation onto the detector.³

There are two principal contributions to the energy resolution of the monochromator. The first derives from the intrinsic angular width of the Bragg reflection in a highly perfect crystal. This finite width, which arises from the finite penetration depth over which the x rays are fully reflected, is called the extinction length and is a function only of the type crystal material (such as silicon or germanium) and the order of the Bragg reflection. For example, for the Si (444) Bragg reflection, the extinction length is 31 microns, which gives an intrinsic energy resolution $\delta(\hbar\omega_1)$ of about 40 meV at $\hbar\omega_1 = 8$ keV. The second contribution derives from the angular spread $\delta\theta$ of the incident synchrotron beam, which by Bragg’s law gives an energy spread $\delta(\hbar\omega_1)/(\hbar\omega_1) = \cot\theta_B \delta\theta$, where θ_B is the Bragg angle for the monochromator. Because $\delta\theta$ is about 0.2 milliradians at current sources like the NSLS, this energy spread is considerably larger than the Si (444) intrinsic width except very near backscattering where $\cot\theta_B \ll 1$. Next-generation synchrotron sources will be much brighter, with smaller beam divergence, and therefore better matched to perfect-crystal monochromators.

With respect to the analyzer, because the inelastic process is incoherent, the scattered radiation is spread out into 4π steradians. One therefore needs an analyzer that collects a relatively large solid angle. However, because the spectrum in the solid changes on a length scale characterized by the spacing of valence electrons (about 2×10^{-8} cm), resolution requirements limit the solid angle to several degrees. The most common setup for a high-energy-resolution (≤ 1 eV) analyzer (as shown in figure 2) consists of a large (about 50 cm²) spherically bent perfect crystal with a 1-m radius of curvature, which does indeed collect a few degrees of solid angle. If the Bragg planes are parallel to the surface of the crystal, then the analyzer can be considered as a spherical x-ray mirror for a single frequency. Thus, the analyzer produces a single-frequency image of the sources at the detector, and the spectrum is obtained by scanning the input frequency. If ω_1 is chosen such that the analyzer crystal backscatters the x rays, the analyzer can have the intrinsic resolution of the crystal. Such a configuration is optimized when the monochromator resolution is matched to the analyzer. Because we are measuring one energy-shift $\hbar\omega$ at a time, the signal is weak, and because in most cases we want many $\hbar\omega$ ’s, an inelastic spectrum can take half a day to collect.



Quantitative aspects of scattering

Although the situation is changing rapidly, there have been only a handful of interesting experiments in valence inelastic scattering. (See figure 3 for an example at large k .) Almost all of these experiments have been done with an absolute energy resolution greater than 1 eV and on low-absorption (low- Z) materials. This modest resolution implicitly limits what we can learn. Despite these shortcomings, we have learned a great deal about the gross electronic structure of a small range of simple materials, but practically nothing about how the electronic excitations at interelectronic distances change when the solid undergoes some type of phase change.

Except for small but interesting magnetic effects, the differential cross section for nonresonant valence inelastic scattering is proportional to the charge dynamic structure factor $S(\mathbf{k}, \omega)$. To discuss the physical behavior of this factor, it is convenient to ask what the spectrum's ω dependence looks like for fixed values of the dimensionless parameter ka , where a is a typical interelectron spacing.

At small momentum transfer ($ka \ll 1$), in the so-called collective regime, the character of the valence inelastic scattering depends on the interference between the scattering amplitudes from many electrons. Because long distances (small k) are important, to get an accurate description of the spectrum we must allow the electron-hole pairs we excite to undergo Coulomb interaction with other electrons in the material. Because the Coulomb interaction is so long ranged, it is never possible to describe valence inelastic scattering at small k without including it. At low momentum transfer, there is a rather accurate microscopic theory called the random phase ap-

COMPTON SCATTERING SIGNATURE AND CARBON PROFILES.

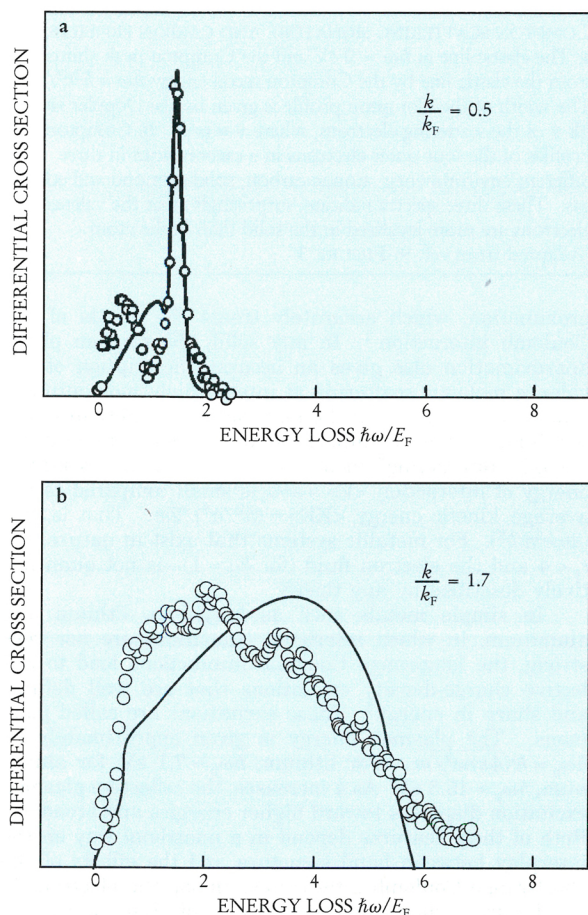
a: The elastic line at $\hbar\omega = 0$ eV and the Compton peak shifted from the elastic line by the Compton recoil energy $\hbar\omega = \hbar^2 k^2 / 2m$. The width of the Compton profile is given by the Doppler shift $\hbar\mathbf{k} \cdot \mathbf{v}$ of the scattering electrons, where $\mathbf{v} \equiv \mathbf{p}/m$. **b:** Compton profiles of the four outer electrons in a carbon atom in three different environments: atomic carbon, solid diamond and ethane gas. These three spectra indicate, surprisingly, that the valence electrons are more localized in the solid than in the atom. (Adapted from ref. 9) **FIGURE 3**

proximation, which accurately treats the effects of the Coulomb interaction.⁴ In any solid, the random phase approximation also gives an accurate description of the valence inelastic scattering at intermediate momentum—that is, when $ka \approx 1$ —if the material is a weakly interacting fluid. For metallic systems at zero temperature, “weakly interacting” means that the average potential energy of interaction $\langle V \rangle \approx e^2/a$ is small compared to the average kinetic energy $\langle KE \rangle \approx (\hbar^2/a^2)/2m$. That is, $r_s = (2me^2a/\hbar^2)$. For metallic systems that exist in nature, $2 < r_s < 4$ and the electron fluid (for $ka \approx 1$)—is not quantitatively described by any theory.

In simple metals such as beryllium, lithium and aluminum, in which interband transitions are not very strong, the long-range Coulomb interactions lead to collective charge-density excitations that are well defined and sharp in energy.⁴ These excitations are called plasmons. The plasmon energy is given approximately by $\hbar\omega_p = \hbar\sqrt{4\pi ne^2/m}$. For lithium, $\hbar\omega_p \approx 7.1$ eV; for aluminum, $\hbar\omega_p \approx 15.3$ eV. As k increases, the collective plasmon excitation disperses toward higher energies and broadens. Both of these features depend in a nontrivial way on the interplay between band structure and the effects of the short-range Coulomb interactions among the electrons.⁵

Figure 4 shows inelastic spectra of aluminum metal for two different momentum transfers⁶ with an energy resolution of 1.5 eV. The energy loss and momentum transfer are shown in terms of the Fermi energy $E_F = 11.6$ eV and Fermi wavevector $k_F = 1.8 \times 10^8/\text{cm}$, respectively. Because aluminum is a free-electron metal, it has a well-defined plasmon, which can be seen in figure 4a at an energy loss of $\hbar\omega/E_F = 1.5$ (17 eV). This feature disperses quadratically with momentum transfer. The curve shows the random phase approximation, which agrees well at the plasmon energy but less well in the lower energy portion of the spectrum, where we expect a bump associated with the low-lying excitations across the Fermi surface. Figure 4b shows a roughly double-bumped feature whose precise physical origin is the subject of some controversy. The spectrum clearly disagrees with the random phase approximation shown by the solid line. It is interesting to note that although crystalline silicon is a semiconductor with a 1-eV bandgap, a corresponding set of spectra would show very similar features with a plasmon at $\hbar\omega \approx 20$ eV. On such a large energy scale, silicon looks like a simple metal with four electrons per silicon atom.

Recently, the first observation of a change in the inelastic spectrum of a solid at small-to-intermediate ka was reported⁷ for the material V_2O_3 . This solid, with a small amount of chromium added to it, undergoes a transition from a paramagnetic metal to an antiferromagnetic insulator at a temperature of 170 K. The spectrum of the insulator is shown in figure 5a. The shoulder on the elastic line and the peak at an energy loss of 9 eV are absent in the metal. The shoulder has been attributed to the opening up of a so-called Mott-Hubbard insulator gap; the second peak seems to be a peculiar kind of exciton that is screened out in the metal. The highest peak



MOMENTUM TRANSFER k DEPENDENCE of the inelastic x-ray spectrum for aluminum. The solid lines in **a** and **b** were calculated by the random phase approximation theory and broadened by the measured resolution function. The plasmon in **a** is broadened by an additional 0.6 eV, accounting for a finite lifetime. (Adapted from ref. 6.) FIGURE 4

present in the metal (figure 5b) and the insulator is a plasmon similar to those seen in figure 4.

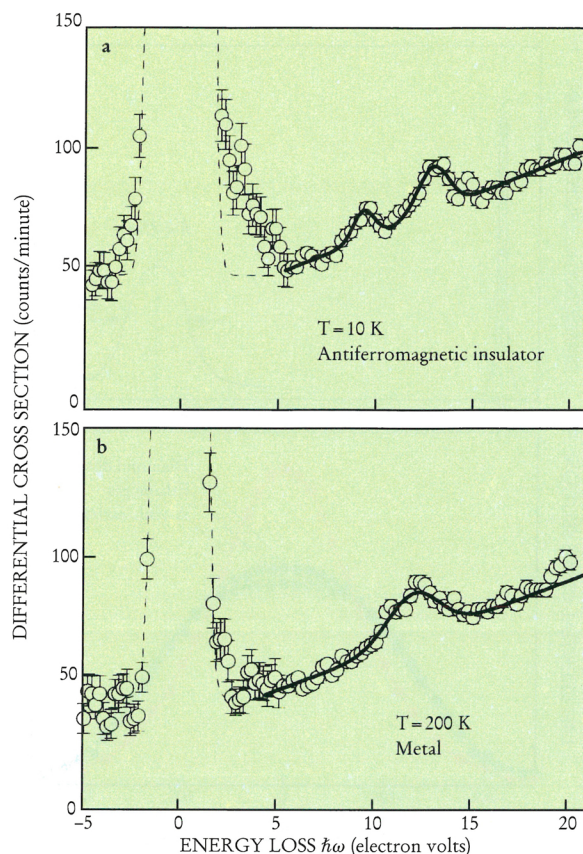
For inelastic scattering at very large momentum transfers ($ka \gg 1$), there is little interference between the scattering amplitudes from different electrons. In this so-called Compton regime, the functional form of $S(\mathbf{k}, \omega)$ is easily discussed because, to an excellent approximation the scattering is from a single representative electron in the solid. It can be shown that the effect of all the other electrons and the ion cores in the solid is to give the scattering electron some probability $n(\mathbf{p})$ of having a momentum \mathbf{p} .

If our single-electron picture were correct, then energy and momentum conservation (recalling that the momentum transfer is $\hbar\mathbf{k}$) would imply that for an electron with momentum \mathbf{p} , the energy transferred is

$$\hbar\omega = (\mathbf{p} + \hbar\mathbf{k})^2/2m - p^2/2m \quad (2)$$

$$= \frac{\hbar^2 k^2}{2m} + \frac{\hbar\mathbf{k} \cdot \mathbf{p}}{m}$$

The quantity $\hbar^2 k^2/2m$ is called the Compton energy shift. It is the recoil shift associated with an electron at rest. The quantity $\mathbf{k} \cdot \mathbf{p}/m = \mathbf{k} \cdot \mathbf{v}$ is naturally called the



TEMPERATURE DEPENDENCE of the inelastic x-ray scattering spectrum in $V_{1.978}Cr_{0.022}O_3$ for $k = 2.1/\text{\AA}$. The solid curves are Gaussian fits to the inelastic spectrum; the dashed curves are fits to the elastic scattering. (Adapted from ref. 7.) FIGURE 5

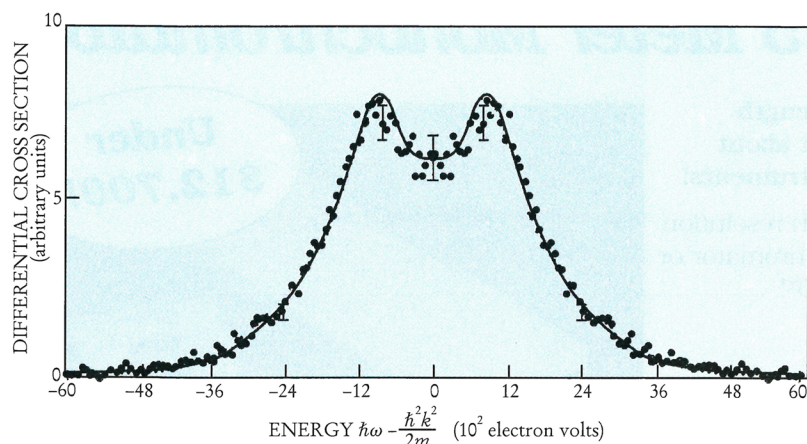
Doppler shift. It is the only part that tells us about the solid.⁸ Roughly speaking, a fixed angle of scattering fixes the momentum transfer, and the shape of the frequency-shifted spectrum centered at $\hbar^2 k^2/2m$ tells us directly the number of electrons with momentum \mathbf{p} that Doppler shift the x rays into that region of phase space.

In the Compton regime, assuming the momentum transfer \mathbf{k} is well defined, the resolution in momentum space is directly proportional to the energy resolution. In particular,

$$\Delta p \approx mc (\Delta\omega_2/\omega_2) \quad (3)$$

Thus, an absolute energy resolution of 1 eV for a 10-keV x ray gives a momentum resolution $\Delta p/\hbar$ of about $2 \times 10^6/\text{cm}$. This is a very good resolution. Equation 3 is the principal reason why many inelastic scattering experiments are done in the Compton regime. Even solid-state detectors with poor energy resolution but high efficiency give momentum resolutions of about $10^8/\text{cm}$, which is good enough for some studies.

Figure 3 shows a Compton inelastic x-ray spectrum for the four outer electrons in a carbon atom when that atom is placed in three different environments: carbon atoms, solid diamond and ethane gas. The atomic spectrum is calculated. The diamond and ethane spectra are directly measured⁹. The details are unimportant. However, the obvious broadening of the profile as one goes



COMPTON PROFILE for a single-crystal sample of itinerant ferromagnetic nickel with \mathbf{k} parallel to the crystallographic $\langle 111 \rangle$ direction. The dip occurs because minority spin-polarized electrons in the ground state are more delocalized in the crystal. The solid line is included as a guide to the eye. (Adapted from ref. 11.) FIGURE 6

from the isolated atom to electrons participating in a covalent bond tells us that the outer electrons in the bond are more localized in real space—that is, more spread out in momentum space (velocity) than those in the atom. A careful analysis of such spectra at a resolution of $2 \times 10^6/\text{cm}$ would give us real insight into subtle electron correlation effects in molecular structures.

If we include the small (1%) relativistic coupling of the x ray to the electron, the magnetic moment of the Compton scattering amplitude can measure the individual spin-up and spin-down momentum distributions.¹⁰ If we line up the magnetization \mathbf{M} , for example, in a ferromagnetic solid and take two Compton profiles, utilizing circularly polarized x rays, one polarized along \mathbf{M} and the other opposite to it, then the difference profile to lowest order in $\hbar\omega_1/mc^2$ is

$$\left. \frac{d\sigma}{d\omega d\Omega} \right|_+ - \left. \frac{d\sigma}{d\omega d\Omega} \right|_- = \sigma_T \left(\frac{\hbar\omega_1}{mc^2} \right) \int (n(\mathbf{p})^\uparrow - n(\mathbf{p})^\downarrow) \delta \left(\hbar\omega - \frac{\hbar^2 k^2}{2m} - \frac{\hbar \mathbf{k} \cdot \mathbf{p}}{m} \right) \quad (4)$$

Figure 6 shows a beautiful magnetic difference profile for the itinerant ferromagnetic material nickel.¹¹ The profile was taken with a resolution of about 0.3 atomic units. This material is interesting because the magnetism comes primarily from itinerant d electrons. These d electrons have wavefunctions that hybridize (mix) with the nonmagnetic, even-more-mobile s and p electrons in the outer shell of the nickel atom in a way that is not yet completely understood. Nevertheless, at least qualitatively in this modest resolution spectrum, we can observe a dip at the center of the profile. This dip is very simply related to the itinerant hybridization band structure picture of the wavefunction. The s and p electrons are the minority carriers—that is, their polarization tends to be opposite that of the d electrons. Because they are more spread out in real space, they are more localized in momentum space than the majority magnetic carriers. Thus the dip in the spectrum.

In the near future, when we are able to measure such profiles with a resolution better than $10^6/\text{cm}$, we should be able to measure changes in the ground-state wavefunction as the system undergoes a phase transition. Some examples include nickel as it passes through its ferromagnetic Curie temperature, high- T_c materials like $\text{La}_{2-x}\text{Sr}_x\text{CuO}_4$ as they pass through their superconducting transition temperature, heavy fermion materials like UPt_3 as they are cooled through their Kondo temperature where the electrons become “heavy” and transition-metal oxides like V_2O_3 as they change from metal to insulator.

For such systems the change in the momentum profile will occur on a scale of momentum $\Delta p/p_F \approx k_B T/E_F$, where E_F is some typical Fermi energy and T is the characteristic temperature at which the transition occurs.

Although there are other methods for measuring ground-state wavefunction properties, none of the existing techniques can be applied to as wide a variety of materials. Nor are they so unambiguously related to a simple bulk ground-state property at atomic distance scales.

Future

Experiments with a resolution better than 0.1 eV are now becoming feasible with the third-generation light sources at Grenoble, Argonne and SPring-8. Such experiments will tell us a great deal about the behavior of electronic excitations as the system changes character. In V_2O_3 , we have one isolated example. It will also be possible to study long-wavelength excitations—phonons in momentum and energy transfer regimes and on samples in which neutrons have difficulties. Such measurements have already been demonstrated in a selected set of low- Z materials such as beryllium and water.¹²

References

1. A. Compton, S. Allison, *X-Rays in Theory and Experiment*, Van Nostrand, Princeton, N. J. (1967).
2. *Handbook on Synchrotron Radiation*, vol. 1B, E. E. Koch, ed., North Holland, New York (1983).
3. C.-C. Kao, K. Hamalainen, M. Krish, D. P. Siddons, T. Overluzen, J. B. Hastings, *Rev. Sci. Instrum.* **66**, 1699 (1995).
4. D. Pines, *Elementary Excitations in Solids*, Benjamin-Cummings, Reading, Mass. (1983).
5. P. Eisenberger, P. M. Platzman, K. C. Pandey, *Phys. Rev. Lett.* **31**, 311 (1973). W. Schulke, H. Nagagawa, S. Mouriki, P. Lanzki, *Phys. Rev. B* **33**, 6744 (1986).
6. P. Platzman, E. D. Isaacs, H. Williams, P. Zschack, G. E. Ice, *Phys. Rev. B* **46**, 12 943 (1992).
7. E. D. Isaacs, P. M. Platzman, J. M. Honig, P. Metcalf, submitted to *Phys. Rev. Lett.*, preprint available from authors.
8. P. M. Platzman, N. Tzoar, *Phys. Rev. B* **2**, 3556 (1970). R. N. Silver, P. E. Sokol, eds., *Momentum Distributions*, Plenum, New York (1989).
9. P. Eisenberger, W. Marra, *Phys. Rev. Lett.* **27**, 1413 (1971).
10. D. M. Mills, *Phys. Rev. B* **36**, 6178 (1987). M. J. Cooper, D. Laundy, D. A. Cardwell, D. N. Timms, R. S. Holt, G. Clark, *Phys. Rev. B* **34**, 5984 (1986).
11. N. Sakai, *Proceedings of the Ninth International Conference on Positron Annihilation*, World Scientific, Singapore (1992).
12. E. Burkel, J. Peisl, B. Dorner, *Europhys. Lett.* **3**, 957 (1987). F. Sette, G. Ruocco, M. Krisch, U. Bergmann, C. Masciovecchio, V. Mazzacurati, G. Signorelli, R. Verbeni, *Phys. Rev. Lett.* **75**, 850 (1995).